Journal of Applied Polymer Science

Effect of ZnO nanoparticles obtained by arc discharge on thermo-mechanical properties of matrix thermoset nanocomposites

C. Medina M,[1,2] D. Rojas,[1] P. Flores,[1,2] E. Peréz-Tijerina,[3] M. F. Meléndrez[1]

[1]Advanced Nanocomposites Research Group (GINA). Hybrid Materials Laboratory (HML). Department of Materials Engineering (DIMAT), Faculty of Engineering, University of Concepción, 270 Edmundo Larenas, Box 160-C, Concepción 4070409, Chile

[2]Department of Mechanical Engineering (DIM), Faculty of Engineering, University of Concepción, 219 Edmundo Larenas, Box 160-C, Concepción 4070409, Chile

[3]Research Center for Physical and Mathematics Sciences, Faculty of Physics and Mathematics, University of Nuevo Leon, Av. Universidad s/n. Ciudad Universitaria 66451, San Nicolás de los Garza Nuevo León, México

Correspondence to: P. Flores (E-mail: pfloresv@udec.cl) and M. F. Meléndrez (E-mail: m.melendrez@udec.cl)

ABSTRACT: Through the development of nanotechnology it has been widely studied the morphology and size control in nanopowders synthesis. However, most of these techniques are successful to synthesize nanopowders in a small scale. In this research, a large semi-industrial scale synthesis method is proposed, named continuous arc discharge in controlled atmosphere (DARC-AC). Using this technique, it is possible to directly obtain clean nanostructures (low amount of impurities) with more than 90% of particles below 100 nm. In this study, the method utilizes metallic zinc and oxygen as precursors in order to produce ZnO. The ZnO nanopowders were incorporated in a thermoset polymer (epoxy resin) to study their influence on the thermo-mechanical properties of the matrix. As main results, the mechanical properties of the nanocomposite epoxy/ZnO nanoparticles (ZnO-NPs) do not differ from the original properties of the epoxy resin. Nevertheless, thermal behavior, conductivity, and diffusivity properties of the nanocomposite are improved. © 2016 Wiley Periodicals, Inc. J. Appl. Polym. Sci. **2016**, *133*, 43631.

KEYWORDS: nanoparticles; nanowires and nanocrystals; properties and characterization; resins; thermal properties; thermosets

Received 24 November 2015; accepted 10 March 2016
DOI: 10.1002/app.43631

INTRODUCTION

The expansion of high performance materials based on epoxy resins have become strategic materials for applications where high thermal stability and environmental resistant are needed.[1] Epoxy resins are mainly used as substrate, coating, or matrix materials for applications in microelectronics, automotive, and transport industry. In general, epoxy resins react with a wide range of curing agents, whereby a highly crosslinked structure is obtained with high stiffness, high glass transition temperature (T_g), and high chemical stability.[2] Through the development of nanotechnology, additional desirable properties have been included to the epoxy systems such as permeability,[3] wear resistance,[4–6] corrosion resistance,[7] and UV resistance.[8] The explanation of this advances are related to the addition of nanoparticles to the epoxy resins, e.g.: TiO_2,[3,4] SiO_2,[5,7,9] Al_2O_3,[10,11] and ZnO.[6,8,12] In particular, the addition of ZnO particles represents high interest due to their good chemical, optical, and biological properties. Besides, ZnO particles are environment friendly.[13]

During the last decade, different efforts have been carried out to produce nanometric metal oxides particles, and several techniques have been widely studied.[14–16] However, most of these techniques are successful to synthesize nanopowders in a small scale. This study aims to synthesize nanoparticles of ZnO by a continuous arc discharge in controlled atmosphere (DARC-AC), which seem to be a promising option to large-scale production of ZnO nanopowders. Using this technique with some inert gas (e.g., Ar or N_2), it is possible to obtain metallic nanopowders of Cu, Zn, Fe, and Al; however if air or oxygen are used then nanostructured metal oxides as Al_2O_3, CuO, ZnO, and Fe_2O_3 are obtained. This is why this technique is dynamic, economical, and versatile for obtaining a semi-industrial scale of this type of nanomaterials.

It has been reported that addition of metal oxide nanopowders in epoxy systems, in particular ZnO nanoparticles, modifies the curing behavior, and crossed-line density, among other properties.[9,17–21] Indeed, Dhoke *et al.*,[12] reported an improvement of the curing behavior from epoxy resin by additions of ZnO nanoparticles. However, Shi *et al.*,[20] demonstrated that the crossed-line density from the epoxy resin decreases with addition of ZnO nanoparticles, due to the sterically hindered

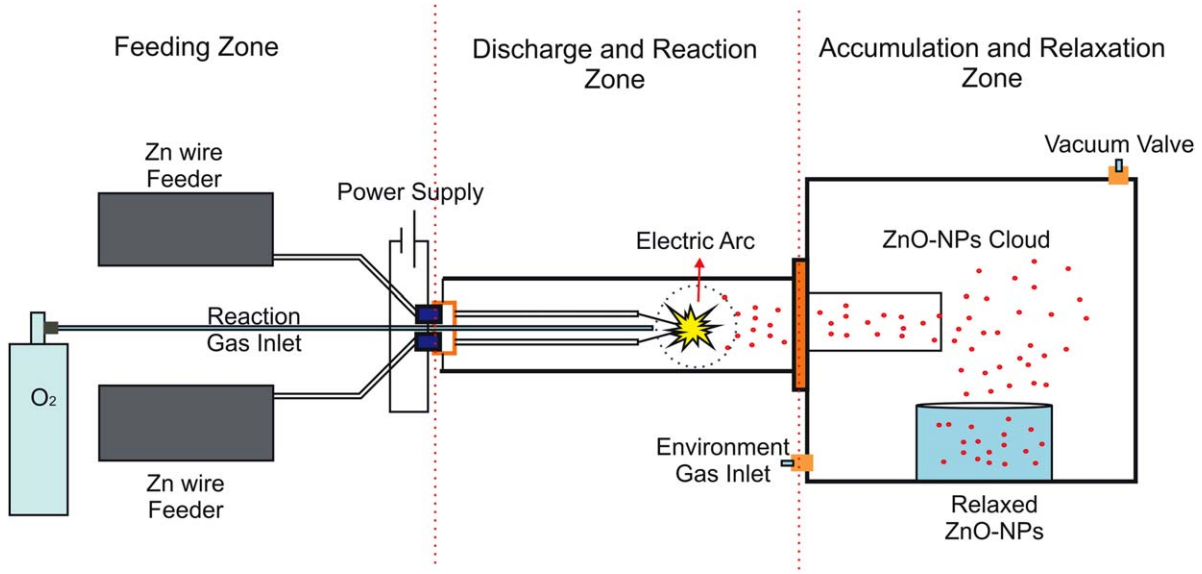

Figure 1. Scheme of synthesis of ZnO-NPs by continuous arc discharge in controlled atmosphere (DARC-AC). The system is divides in three zones: feeding zone, discharge zone, and accumulation zone. [Color figure can be viewed in the online issue, which is available at wileyonlinelibrary.com.]

reaction between the functional groups owing the presence of ZnO nanopowders. This phenomenon is reflected in changes of the glass transition temperature (T_g) and the mechanical properties of the composite material.

To study the multifunctionality of the nanocomposites, the characterization plays a fundamental role. In this particular case, several tests such as dynamic mechanical analysis (DMA), differential scanning calorimetry (DSC), thermal conductivity test, and nanoindentation, were carried out to clarify the influence of the ZnO nanoparticles in the thermo-mechanical properties. Nanoindentation analysis has become an indispensable tool to carry out adequate mechanical characterization of nanocomposites, owing the traditional mechanical tests require large samples and the influence of the nanoparticles on the composite material it is not perceptible in the macrometric scale.[22–24]

This research is based on the study of the thermo-mechanical properties of an epoxy system modified by ZnO nanoparticles. The ZnO nanoparticles were produced by a continuous arc discharge in controlled atmosphere (DARC-AC) technique, which seem to be a promising method to synthesize nanopowders in a semi-industrial scale.

EXPERIMENTAL

ZnO-NPs Synthesis

The continuous arc discharge in controlled atmosphere (DARC-AC) is a continuous physical vapor deposition technique, where a thin wire used as metallic precursor, is vaporized by a strong electric arc discharge. In the process, the metallic wire is fed to the system at constant rate. Due to the high current that passes through the wire, a continuous arc is produced. As result, the metallic precursor transforms in a superheated vapor cloud, which expands, collides with atmosphere's molecules, and cools down to produce homogeneous nucleation of nanoparticles.

The Figure 1 shows the device used to produce the nanoparticles. This device is divided in three zones: (1) feeding zone, where the Zn wire and the gas is supplied; (2) discharge and reaction zone, where the arc discharge takes place; and (3) accumulation and relaxation zone, where the synthesized nanoparticles are stored. The nanoparticles are produced in the discharge and reaction zone, after they are carried by the reaction gas to the accumulation and relaxation chamber.

To produce the nanoparticles, commercial high purity a 2 mm diameter Zn wire (99.99% Zn) from Sulzer (Winterthur, Switzerland) was used as metallic precursor and oxygen as gaseous precursor with a flow of 500 sccm. The operating voltage and current were 25 V and 30 A, respectively. The arc inclination angle was 40° with an electrode distance of 0.5 cm and speed precursor's wires was 0.5 cm/s. The reaction was conducted at 1 atm and both the reaction and accumulation chambers were enriched with oxygen prior to discharge.

The reaction of precursors by the arc discharge was carried out by pulses, in order to avoid the reactor overheating. The nanoparticles cloud continue to the accumulation and relaxation chamber, where they require 60 min as relaxation time, after that the nanoparticles are recollected in the bottom of the chamber which is filled by an inert atmosphere.

Nanocomposite Preparation

The thermostable matrix was prepared with an epoxy resin (prepolymer) of Bisphenol A (epichlorhydrin) and a curing agent composed of three crosslinked agents; 3-aminomethyl-3,5,5-trimethyl cyclohexamine, 5-amino-1,3,3-trimethylcyclohexanemethanamine, and triethylenetetramine. Both resin and curing agent were purchased from R&G (composite technology, Waldenbuch, Germany). The resin used to prepare the nanocomposites presented low viscosity, which it is appropriate to facilitate dispersion of the nanoparticles.

The dispersion quality of the filler in the matrix has an important influence on the mechanical properties of nanocomposites. It has been reported[24,25] that a good dispersion of

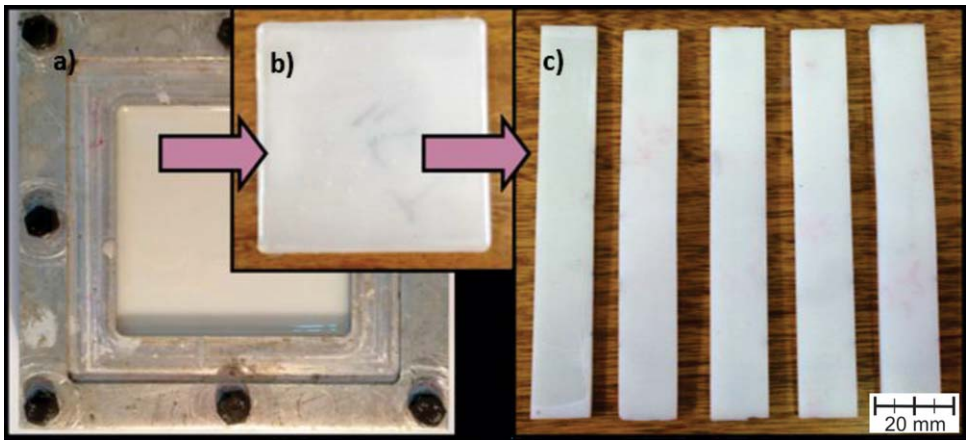

Figure 2. (a) Preparation of nanocomposite in open mold. (b) Nanocomposite with thermostable matrix. (c) Samples to perform thermo-mechanical tests (DMA). [Color figure can be viewed in the online issue, which is available at wileyonlinelibrary.com.]

nanoreinforcements improves the mechanical properties of pure epoxy resin, while agglomeration of nanoreinforcements originate voids that decrease the mechanical properties. Therefore, a crucial stage in preparation of the nanocomposites is to achieve a good dispersion of the filler in the matrix. For that reason, the filler incorporation process (ZnO nanoparticles, ZnO-NPs) into the matrix was separated in three steps. First, mechanical stirring was carried out to the mixture between the epoxy system and the nanoparticles at 500 RPM by 30 min. Subsequently, the mixture was exposed to ultrasonic cavitation with variable pulse by 10 min, in order to avoid agglomeration. Finally, to ensure homogeneity and refinement, the mixture was passed through a three-roll mill, where separation between the first and the second roller was set at 0.15 mm, while the separation between the second and third roller was set at 0.07 mm. The rate used in the three-roll mill process varied from 30 RPM to 130 RPM increasing by 10 RPM after each cycle.

To prepare the nanocomposites, the epoxy resin with ZnO-NPs was mixed with the curing agent and degassed by ultrasonic cavitation. To facilitate the curing, the mixture was poured into an open mold (100 ×100 mm) where was kept at ambient temperature for 24 h, followed by a post-curing process at 100 °C for 15 h in a muffle furnace. Figure 2(a) shows the nanocomposite in the mold. The nanocomposite presented a homogeneous matrix without any decantation process in the samples nether voids or bubbles that could decrease the material properties [Figure 2(b)]. Figure 2(c) shows the cuts of the nanocomposite plate to perform thermo-mechanical tests.

In order to evaluate the effect of different filler concentrations in the thermo-mechanical properties of the nanocomposite, several samples were prepared with different concentration of nanoparticles (0%, 0.3%, 0.5%, 0.8%, 1.0%, and 2.0% weight percent). The configurations of the prepared samples are shown in the Table I.

CHARACTERIZATION

Structural and Morphological Characterization

High-resolution transmission electron microscopy (HRTEM) was performed in a JEM-ARM200F probe aberration corrected analytical microscope with a resolution of 0.08 nm. Selected area electron diffraction was performed in a JEOL 2010F operating at 200 kV (point resolution of 0.19 nm). Scanning electron microscopy (SEM) was carried out using a FEG Hitachi S-5500 ultra high-resolution electron microscope (0.4 nm at 30 kV) with a BF/DF Duo-STEM detector and in a FEI-Nanonova 100 FESEM.

Thermo-Mechanical Characterization

Dynamic mechanical thermal analysis was performed in a DMA Q800 (TA instruments) with single cantilever configuration. Testing conditions were: temperature 30–250 °C, frequency 1 Hz, deflection 30 micron, and temperature slope 3 °C/min. Differential scanning calorimetry was performed in a DSC Q200 (TA instruments), with temperature from 20 to 220 °C and temperature slope 10 °C/min.

A Hysitron TI 950 triboindenter with Berkovich tip was used for nanoindention. The testing speed (Tsp) was 25 nm/s and maximum load was 12,000 μN. Elastic modulus and hardness were calculated from load/displacement curve, according to Oliver and Pharr method.[26]

Thermal Characterization

Using a transient plane source technique (TPS) with double spiral sensor, the thermal properties were measured. Thermal conductivity and thermal diffusivity were performed in a hot disk thermal constants analyzer. The testing conditions were:

Table I. Configuration of Prepared Samples with Different Amount of ZnO-NPs

Configuration	Material
E1	Neat epoxy
Z1	Epoxy + ZnO-NPs 0.3% wt.
Z2	Epoxy + ZnO-NPs 0.5% wt.
Z3	Epoxy + ZnO-NPs 0.8% wt.
Z4	Epoxy + ZnO-NPs 1.0% wt.
Z5	Epoxy + ZnO-NPs 2.0% wt.

The configuration E1 refers to epoxy resin without ZnO-NPs.

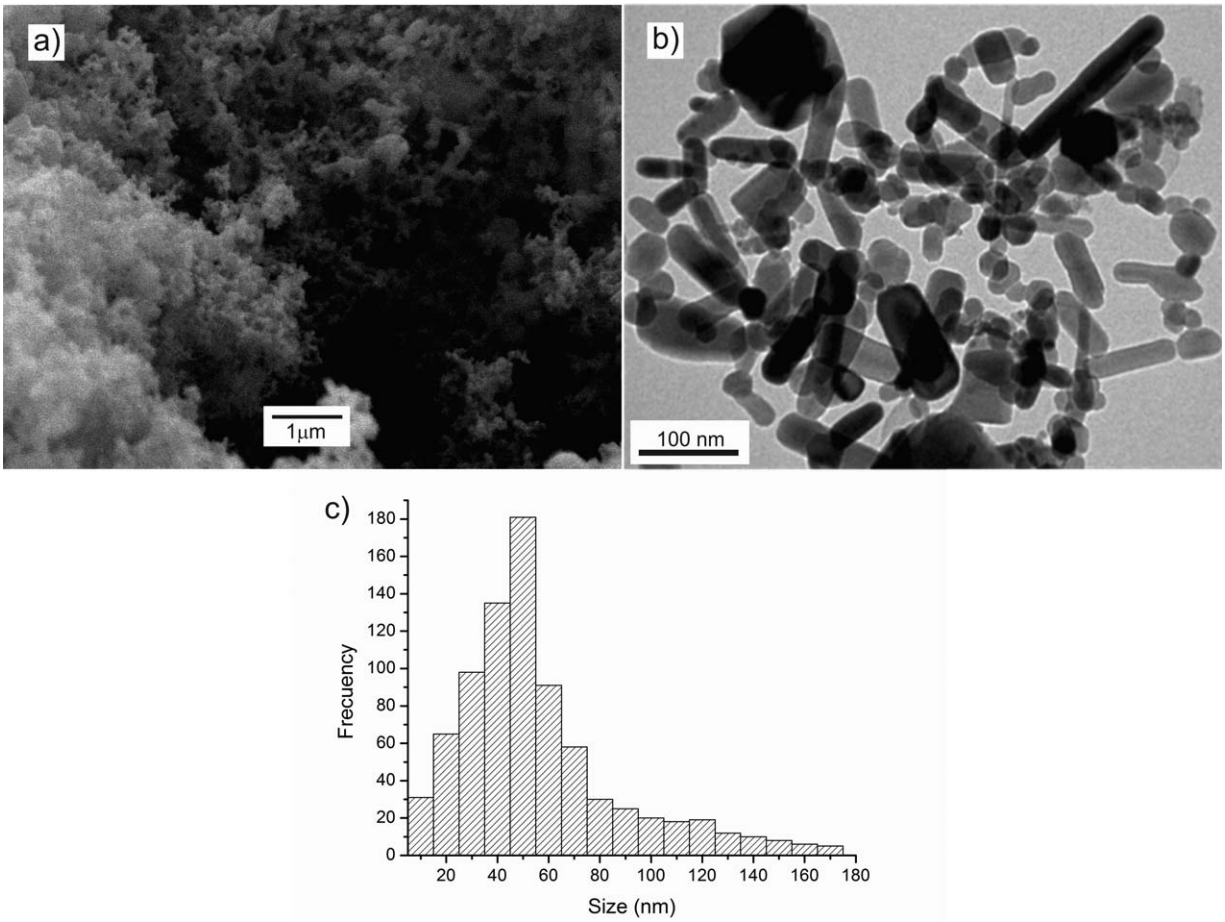

Figure 3. (a) SEM low magnification image showing obtained nanoparticles after the DARC-AC process. (b) TEM image indicating nanoparticles morphology and size. (c) Frequency particles size histogram.

measured depth 3 mm, room temperature 20 °C, power output 0.05 W, measuring time 20 s, and Kapton sensor with 4 mm diameter.

RESULTS AND DISCUSSION

Synthesis

The DARC-AC synthesis technique was used to the massive production of ZnO-NPs in a simple and economical manner. The precursors materials used in this production method do not generate sub-products during the synthesis of ZnO nanoparticles, which is reflected in high the efficiency of process (about 95%). The reaction residues are separated in different chambers to avoid the contamination of produced ZnO-NPs.

The synthesis process results are shown in Figure 3(a–c). Figure 3(a) shows a low magnification SEM image where it is possible to observe the massive production of ZnO-NPs. The nanoparticles morphology is presented in Figure 3(b), with prismatic and rod morphology showing different particle diameter (Transmission electron microscopy image). The reaction related to this method produced high amount of synthesized material. However, the particles size distribution had a wide range of particle distribution.

The particles size distribution is shown in the frequency histogram [Figure 3(c)]. The main particle type obtained in the synthesis showed prismatic morphology, with particles width from 15 nm to 180 nm in the minor semi axis. The average particles size considering prismatic morphology was about 56 nm.

The advantages of this technique compared to others, is its high level of crystallization of nanostructures without using further heat treatment, the large amount of obtained material and its purity. Its main disadvantage is the wide size distribution obtained. Si *et al.*,[27] used a discontinuous arc discharge synthesis method to obtain Gd nanoparticles with an average size of 40 nm, the problem of the discontinuous arc configuration was that residues of the synthesis were mixed with nanoparticles and for this reason, the purity of the product was poor. Furthermore, the authors in refs. 28–31, synthesized nanoparticles of different materials such as Mn, Ag, and ZnO, using fixed electrodes in frontal position. However, the synthesis problem was that the final mixture was contaminated with reaction residues, decreasing the final product quality.

It is noteworthy that has not been reported to semi-industrial scale production by this technique (arc discharge in a controlled atmosphere). For this reason, the technique is effective to produce large scale of nanopowders, with high purity and high crystallinity level of the product. Table II summarizes the main

Table II. Comparison between Different Nanoparticles Synthesis Process

Method	Advantages	Disadvantages
CVD	High deposition rate	High vapor pressure
SOL-GEL	Large areas	Expensive precursors
PVD	No chemical substances	Low deposition rate
Mechanical grinding	Any metal	High impurities
Arc-discharge	High crystallinity	Broad distribution size

advantages and disadvantages of obtaining nanomaterials using some physical and chemical methods of synthesis.

The X-ray Diffraction (XRD) analysis [Figure 4(a)] revealed that ZnO-NPs presented hexagonal Wurtzite crystallographic structure (JCPDS 75-0576) (a = 0.3249 nm, c = 0.5205 nm).[32] In the spectrum, was not found any peak related with metallic Zn. Therefore, the contamination possibility of ZnO-NPs with metallic Zn coming from the precursor wire was discarded.

Figure 4(b) shows a HRTEM image where it is possible to observed the preferential disposition of the atomic arrangement and the indexation diffraction pattern. It has been reported[33] that the ZnO-NPs usually grows on (001) direction, which it is in agreement with the figure. The FFT analysis was used to calculate an interplanar distance of 0.26 nm related to (002) planes, which confirm the XRD results. Moreover, the obtained results from HRTEM and XRD discard the possibility of crystalline defects formation and confirm that the DARC-AC technique is able to synthesize ZnO-NPs in a massive and simple manner.

Thermo-Mechanical Characterization

The Table III shows the glass transition temperature (T_g) results, obtained by DSC and DMA (Tan δ) thermal analysis related to all sample configurations (Table I). These results showed a slight increment on the glass transition temperature of the epoxy/ZnO-NPs systems in comparison to the pure epoxy resin. It has been reported[15] that the T_g depends on the crosslinking degree of resin chains and the physical interaction between the nanoparticles and the matrix. Shi et al.[20] have explained that addition of ZnO-NPs to the matrix presented a negative effect on the crosslinking density and curing process, which showed an increment in the viscosity of the mixture due to the nanoparticles. Moreover, an increment in the viscosity together with a steric effect of the nanoparticles caused a decrease on the curing degree thus a decrease in the crosslinking density and the T_g.[15,16] Nevertheless, Karasinski *et al.*[21] and Dhoke *et al.*[12] studied the curing kinetic of an epoxy/ZnO system, they have shown that it is possible to obtain a higher curing degree by the addition of ZnO-NPs, which also generated an increment in the crosslinking degree and the T_g. In the author's point of view, the T_g depends on the crosslinking degree and in the chains mobility. Therefore, to the author's opinion the addition of ZnO-NPs to the matrix produced obstacles to chains mobility in the epoxy net, which is reflected in a slight increment of the T_g. Nevertheless, this increment on T_g results reported in Table III are negligible, because is below 5%.

The storage modulus obtained by the DMA is shown in Figure 5(a). In the Table III, a slight increment on the storage modulus is observed due to the addition of the ZnO-NPs to the epoxy system. In the rubber zone, where the resin's elastic modulus is lower, is possible to observe a greater influence of ZnO-NPs [Figure 5(b)], because the increased temperature allows the polymer chains relaxation, then the storage modulus increase is due to the addition of nanomaterial. However, the scatter of the elastic modulus at room temperature is just about of 6% between all obtained results. Therefore, the effect of ZnO-NPs in the epoxy resin can be neglected.

The elastic modulus and hardness measurements were determined by nanoindentation technique (Table III). Figure 6(a)

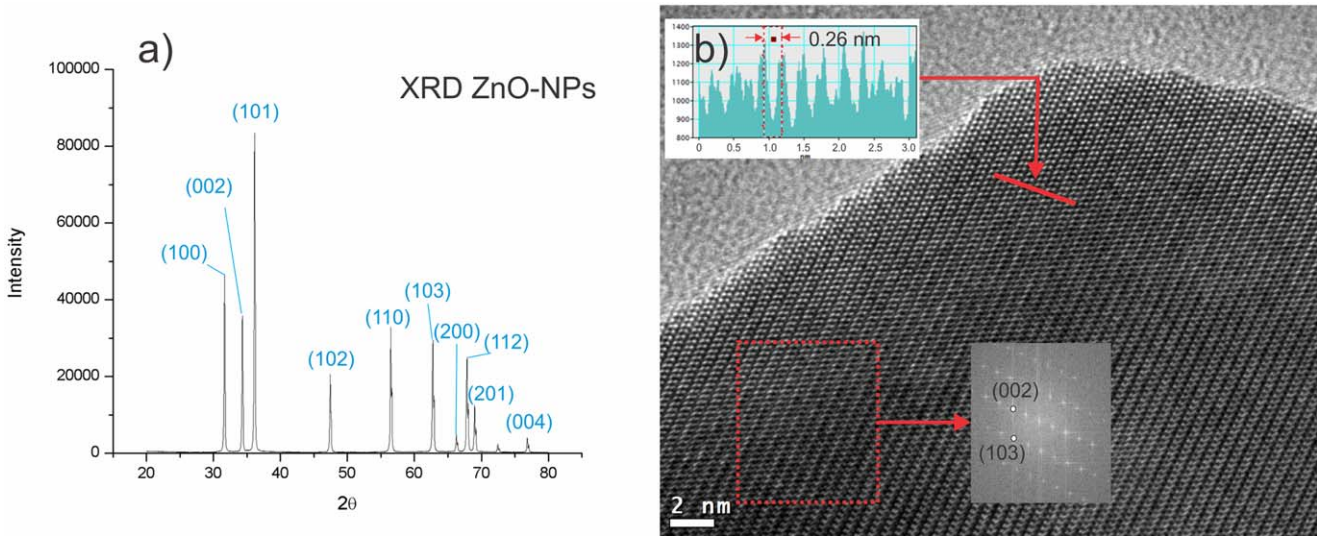

Figure 4. (a) XRD spectrum, the indexation of the peaks shows that the ZnO-NPs have a hexagonal wurtzite type crystallographic structure (b) HRTEM image of ZnO-NPs, shows crystalline structure of obtained ZnO-NPs and preferential growing on direction [001]. [Color figure can be viewed in the online issue, which is available at wileyonlinelibrary.com.]

Table III. Thermo-Mechanical Properties of the Nanocomposites Based on ZnO-NPs and Epoxy Resin

Code	T_g (°C)	Peak tan delta (°C)	Storage modulus (30°C) (MPa)	Storage modulus rubber zone (MPa)	Elastic modulus (GPa)	Hardness (GPa)
E1	96.70	119.21	2182	21.43	3.45 ± 0.02	0.188 ± 0.002
Z1	100.77	119.68	2185	22.20	3.47 ± 0.10	0.190 ± 0.002
Z2	98.47	119.31	2224	22.51	3.42 ± 0.14	0.190 ± 0.002
Z3	99.88	120.86	2126	22.79	3.43 ± 0.06	0.191 ± 0.002
Z4	98.94	119.74	2262	23.10	3.46 ± 0.07	0.192 ± 0.002
Z5	102.10	120.63	2186	23.47	3.45 ± 0.08	0.191 ± 0.002

shows the elastic modulus and hardness results, both tests presented about 2% of variation between the maximum and minimum obtained value. The obtained results are in agreement with the literature,[15,16,21] which suggest that the effect of addition of the ZnO-NPs to the epoxy resin is negligible. In rigid polymers that generally have values above 2.5 GPa, the addition of a low percentage of nanoparticles, does not influence on the elastic modulus of the nanocomposite.[34] In our case, the elastic modulus measured for neat epoxy resin was 3.45 GPa, which explained the null effect of ZnO-NPs. Regarding the hardness, Figure 6(a) shows an increasing trend, this is because the additional material supports the polymer chains to prevent penetration, increasing the hardness, and however the variation is negligible.

All the obtained results showed experimental dispersion, being more notorious in the nanocomposites, in comparison to the pure epoxy resin. The scatter in the elastic modulus and hardness measurement obtained by nanoindentation is related to the specific zones where the measurements were carried out. Local zones free of nanoparticles, with agglomeration of nanoparticles or good distribution of nanoparticles, shall present wide scatter in the measurements.

Thermal Characterization

To improve the thermal conductivity of polymer composites, Ekstrand *et al.*[35] proposed three methods, such as (1) decrease the number of thermally resistant joints; (2) form conductive networks; (3) minimize interfacial defects between matrix and nanoparticles. Fu *et al.*[36] studied the thermal conductivity of nanocomposites with resin and different types and concentrations of nanoparticles, including the ZnO. They informed that it is possible to obtain an increment from 0.2 to 0.8 W/mK with 66% of nanoparticles (weight percent). They concluded that the increment on the thermal conductivity is related to the conductive network formed by the nanoparticles, together to the reduction of the thermally resistant joints. Peng *et al.*[14] obtained similar results mixing ZnO nanoparticles and ZnO nanorods. According to the transient plane source (TPS) results [Figure 6(b)], the addition of ZnO nanoparticles caused a decrease of the thermally resistant

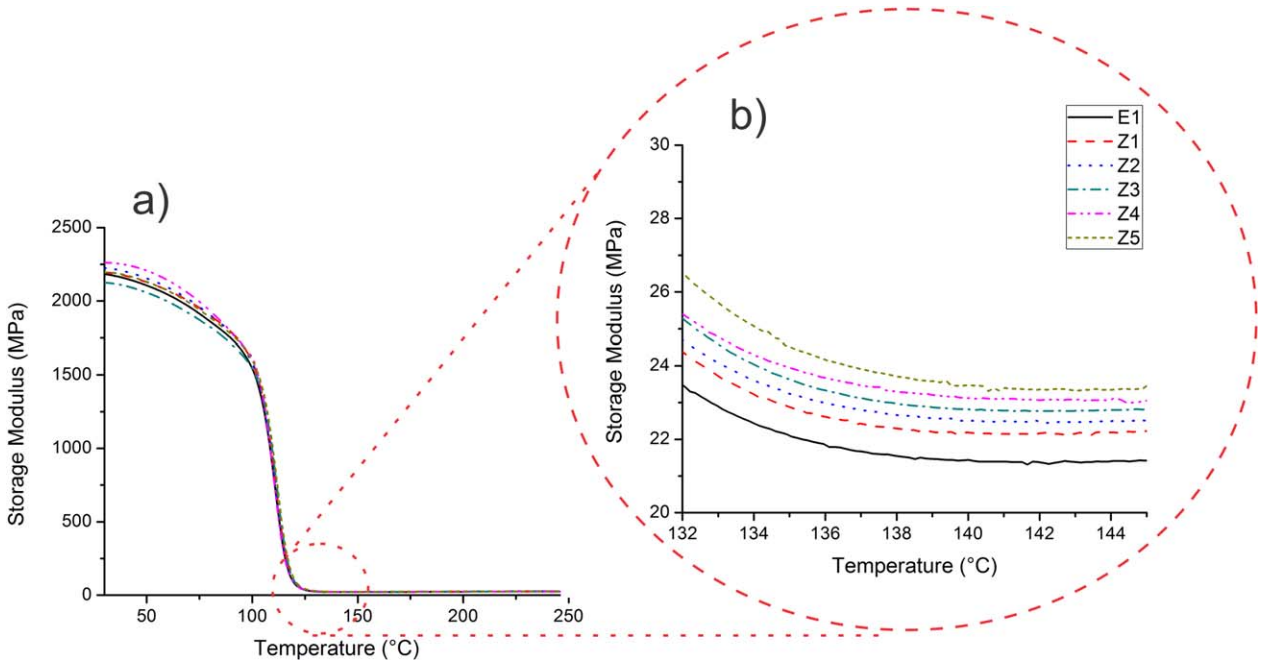

Figure 5. (a) Storage modulus obtained by DMA and (b) nanocomposites storage modulus in rubber zone. [Color figure can be viewed in the online issue, which is available at wileyonlinelibrary.com.]

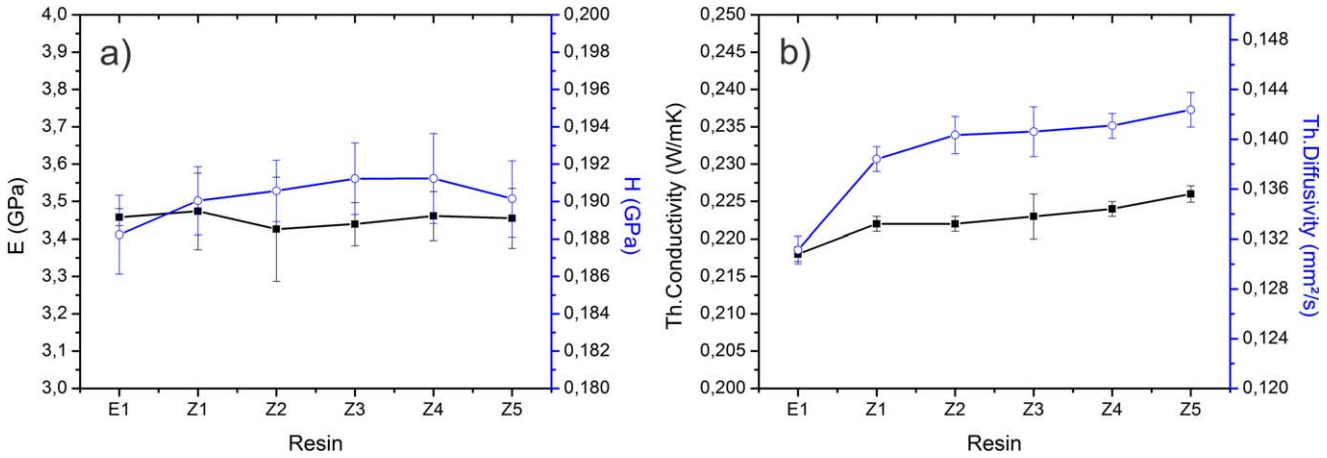

Figure 6. (a) Elastic modulus and hardness obtained by nanoindention. (b) Nanocomposites thermal conductivity and thermal diffusivity. [Color figure can be viewed in the online issue, which is available at wileyonlinelibrary.com.]

joints. However, the amount of nanoparticles in the system (less than 2%), was not enough to form the conductive networks. Therefore, an increment on the thermal conductivity of 3.5% was observed (from 0.218 to 0.226 W/mK). Despite of the high thermal conductivity of ZnO-NPs (about 60 W/nK), there is a high thermal resistance between the ZnO-NPs and the epoxy matrix. Han *et al.*[37] explained this behavior considering that the ZnO-NPs present an "island" effect with few conductive paths, due to a good dispersion of the nanoparticles in the epoxy system. Moreover, nanocomposites, which presented agglomeration of nanoparticles, showed higher thermal conductivity than nanocomposites with a good dispersion, due to the formation of percolated networks. Regarded the thermal diffusivity, a similar explanation was proposed.

CONCLUSIONS

The continuous arc discharge in controlled atmosphere method (DARC-AC), allows a massive, continuous, and economical manner to synthesize nanoparticles with high efficiency (about 95%) and low amount of contamination of the nanoparticles by subproducts.

Despite of DARC-AC technique shows a wide range of particle distribution, near to 90% of particles size considering prismatic morphology were less than 100 nm according to frequency histogram analysis.

The addition of the ZnO-NPs to the epoxy resin caused a slight modification on the glass transition temperature (T_g), which could be explained by the pinning of polymer chains by the nanoparticles, obstructing the free movement of polymer chains.

The mechanical property of the epoxy/ZnO-NPs nanocomposite does not differ from the mechanical properties of the pure epoxy resin. However, an improvement on the thermal properties, such as conductivity and diffusivity of the nanocomposite are observed.

ACKNOWLEDGMENTS

The authors would like to thank the financial support to this work from FONDEF CA12i10308 and CONICYT Regional (CIPA/R08C1002), the National Commission for Scientific and Technological Research, CONICYT No. 21110094 – Ministry of Education, Government of Chile. Additionally, the authors gratefully acknowledge the support of the electronic microscopy laboratory of the International Center for Nanotechnology and Advanced Materials at the University of Texas in San Antonio, the IMDEA materials institute of Madrid, Spain, and the Advanced Nanocomposites Research Group (GINA) at the Materials Engineering Department (DIMAT), University of Concepción, Concepción, Chile.

REFERENCES

1. Thomas, R.; Yumei, D.; Yuelong, H.; Le, Y.; Moldenaers, P.; Weimin, Y.; Czigany, T.; Thomas, S. *Polymer* **2008**, *49*, 278.
2. Gowda, S. K. N.; Mahendra, K. N. *Bull. Korean Chem. Soc.* **2006**, *27*, 1542.
3. Radoman, T. S.; Džunuzović, J. V.; Jeremić, K. B.; Grgur, B. N.; Dejan, S.; Miličević, D. S.; Popović, I. G.; Džunuzović, E. S. *Mater. Des.* **2014**, *62*, 158.
4. Dasari, A.; Yu, Z. Z.; Mai, Y. W. *Mater. Sci. Eng.* **2009**, *63*, 31.
5. Jia, Q. M.; Zheng, M.; Xu, C. Z.; Chen, H. X. *Polymer Adv. Tech.* **2006**, *17*, 168.
6. Sanes, J.; Carrión, F. J.; Bermúdez, M. D. *Wear* **2010**, *268*, 1295.
7. Chang, K. C.; Lin, H. F.; Lin, C. Y.; Kuo, T. H.; Huang, H. H.; Hsu, S. C.; Yeh, J. M.; Yang, J. C.; Yu, Y. H. *J. Nanosci. Nanotechnol.* **2008**, *8*, 3040.
8. Li, Y. Q.; Fu, S. Y.; Mai, Y. W. *Polymer* **2006**, *47*, 2127.
9. Baller, J.; Becker, N.; Ziehmer, M.; Thomassey, M.; Zielinski, B.; Muller, U.; Sanctuary, R. *Polymer* **2009**, *50*, 3211.
10. Naous, W.; Yu, X. Y.; Zhang, Q. X.; Naito, K.; Kagaw, Y. *J. Polym. Sci. B* **2006**, *44*, 1466.
11. Cayton, R.; Brotzman, R. W. *MRS Symp. Proc.* **2001**, *8*, 703.
12. Dhoke, S. K.; Khanna, A. S.; Mangal Sinha, T. J. *Progr. Org. Coat.* **2009**, *64*, 371.

13. Mostafaei, A.; Nasirpouri, F. *Progr. Org. Coat.* **2014**, *77*, 146.
14. Chenmin, L; Dong, L; Xianxin, L; Choi, A; Lee, PWM: Effects of surface treatments on the performance of high thermal conductive die attach adhesives (DAAs). Electronic Materials and Packaging (EMAP), 2012 14th International Conference on; 13–16 Dec. **2012**, 1–5.
15. Ramezanzadeh, B.; Attar, M. M.; Farzam, M. *Progr. Org. Coat.* **2011**, *72*, 410.
16. Ramezanzadeh, B.; Attar, M. M.; Farzam, M. *J. Therm. Anal. Calorim.* **2011**, *103*, 731.
17. Fraga, F.; Soto, V. H.; Rodriguez-Nunez, E.; Martinez-Ageitos, J. M.; Rodriguez, V. *J. Therm. Anal. Calorim.* **2007**, *87*, 97.
18. Sharma, P.; Choudhary, V.; Narula, A. K. *J. Therm. Anal. Calorim.* **2008**, *94*, 805.
19. Germinario, L. T.; Shang, P. P. *J. Therm. Anal. Calorim.* **2008**, *93*, 207.
20. Shi, H.; Liu, F.; Han, E.; Wei, Y. *J. Mater. Sci. Technol.* **2007**, *23*, 551.
21. Karasinski, E. N.; Da Luz, M. G.; Lepienski, C. M.; Coelho, L. A. F. *Thermochim. Acta* **2013**, *569*, 167.
22. Lee, H.; Mall, S.; He, P.; Shi, D.; Narasimhadevara, S.; Yeo-Heung, Y.; Shanov, V.; Schulz, M. J. *Compos. B* **2007**, *38*, 58.
23. Sánchez, M.; Rams, J.; Campo, M.; Jiménez-Suárez, A.; Ureña, A. *Compos. B* **2011**, *42*, 638.
24. Hiroaki, M.; Lawrence, T. D. *Polymer* **2004**, *45*, 5163.
25. Shi, D.; Lian, J.; He, P.; Wang, L. M.; Xiao, F.; Yang, L.; Shulz, M. J.; Mast, D. B. *Appl. Phys. Lett.* **2003**, *83*, 5301.
26. Oliver, W. C.; Pharr, G. M. *J. Mater. Res.* **1992**, *7*, 1564.
27. Si, P. Z.; Brück, E.; Zhang, Z. D.; Tegus, O.; Zhang, W. S.; Buschow, K. H. J.; Klaasse, J. C. P. *Mater. Res. Bull.* **2005**, *40*, 29.
28. Si, P. Z.; Škorvánek, I.; Kováč, J.; Geng, D. Y.; Zhao, X. G.; Zhang, Z. D. *J. Appl. Phys.* **2003**, *94*, 6779.
29. Lee, J. G.; Li, P.; Choi, C. J.; Dong, X. L. *Thin Solid Films* **2010**, *519*, 81.
30. Ashkarran, A. *Curr. Appl. Phys.* **2010**, *10*, 1442.
31. Sönmezoglu, S.; Eskizeybek, V.; Toumiat, A.; Avcı, A. *J. Alloy Comp.* **2014**, *586*, 593.
32. Sun, X. M.; Chen, X.; Deng, Z. X.; Li, Y. D. *Mater. Chem. Phys.* **2003**, *78*, 99.
33. Melendrez, M. F.; Hanks, K.; Leonard-Deepak, F.; Solis-Pomar, F.; Martinez-Guerra, E.; Pérez-Tijerina, E.; Jose-Yacaman, M. *J. Mater. Sci.* **2012**, *47*, 2025.
34. Ci, L.; Bai, J. *Compos. Sci. Technol.* **2006**, *66*, 599.
35. Ekstrand, L.; Kristiansen, H.; Liu, J. **2005**. "Characterization of Thermally Conductive Epoxy Nano Composites", IEEE 28th International Spring Seminar on Electronics Technology: Meeting the Challenges of Electronics Technology Progress; Wiener Neustadt, Austria, 19–23.
36. Fu, Y. X.; He, Z. X.; Mo, D. C.; Lu, S. S. *Appl. Therm. Eng.* **2014**, *66*, 493.
37. Han, Z.; Wood, J. W.; Herman, H.; Zhang, C.; Stevens, G. C. "Thermal Properties of Composites Filled With Different Fillers", IEEE International Symposium on Electrical Insulation; Vancouver, Canada, 497–501.